Journal of Engineering Research and Applied Science
Available at www.journaleras.com
Volume 11 (2), December 2022, pp 2111-2122
ISSN 2147-3471 © 2022

Petrographic and Geochemical characteristics of Paleozoic Gabbroic rocks around Taşdelen (Özdil / Trabzon, NE Türkiye)

Abdullah Kaygusuz

Gümüşhane University, Geological Engineering, Gümüşhane, Turkey

Accepted 28 October 2022

Abstract

The Esatern Pontides comprises many plutonic rocks varying in age, composition and size from Paleozoic to Tertiary. Although those of especially Carboniferous aged ones from these plutonic rocks are widely observed as large bodies in the southern zone of the Eastern Pontides, they are less common in the northern zone and consist of smaller bodies. In this paper, Carboniferous aged Taşdelen Gabbroic rocks were investigated petrographically and geochemically. The Taşdelen Gabbroic rocks mainly consist of plagioclase, pyroxene, hornblende and Fe-Ti oxide minerals. They are calc-alkaline in characters and have low-K content. The samples have metalluminous characters and have low SiO_2 contents (47-49 wt%). They are enriched in-large ion lithophile (LILEs) and light rare earth elements (LREEs) and depleted in high-field strength elements (HFSEs). Chondrite-normalized rare earth element distributions are characterized by concave-upward shapes (La_N/Yb_N = 2.59 to 3.07) and show slightly positive to negative Eu anomalies (Eu_N/Eu^* = 0.97 to 1). All these features demonstrate that the studied gabbroic rocks may have been derived from partial melting of lithospheric mantle.

Keywords: Taşdelen Gabbro, Whole-rock Geochemistry, Lithospheric mantle, Özdil (Trabzon), NE Türkiye

1. Introduction

The Eastern Pontides (NE Türkiye), located in the Alpine-Himalayan orogenic belt and also known as the eastern part of the Sakarya Zone, is one of the important areas where plutonic and volcanic rocks are commonly observed [1–9].

The Eastern Pontides comprise many plutonic rocks, varying from gabbro to granite in compositions, with a wide range of age varying from Early Cambrian to Eocene (Figure 1). These plutonic rocks intruded mainly at five different time periods including Early Cambrian, Carboniferous, Jurassic, Cretaceous and Eocene (Figure 1). Early Cambrian plutons intruded into the metasedimentary rocks [10], Paleozoic plutons intruded into the metamorphic rocks [11–19], Jurassic plutons intruded into the Early Jurassic volcano-sedimentary rocks [20,21], Cretaceous plutons intruded into the subduction-related volcanic rocks [4–6,22–25], and Eocene and later plutons are intruded all former units [7,23,25–30].

Despite the petrological and geochemical studies have been conducted on Carboniferous plutons in the region [13–19,32,33], no study has been conducted on the petrographic, geochemical and petrological properties of the Taşdelen Gabbroic rocks, and were first demonstrated by this study.

2. Regional geology and Geological Setting

The oldest basement rocks in the Eastern Pontides consist of Neoproterozoic metasedimentary rocks [34] and these basement rocks were cut by Early Cambrian metagranitoid [10]. Early Carboniferous metamorphic rocks [35] come on these rocks and they were cut by Late to Early Carboniferous Plutonic rocks [13–18,32]. These Pre-Jurassic basement rocks are overlain by the Early and Middle Jurassic volcano-sedimentary rocks [36–38] and are cut by Mid to Late Jurassic plutons [20,21,39]. All these units are overlain by the Late Jurassic to Early Cretaceous carbonates [40]. The Late Cretaceous units that unconformably overlie these carbonate rocks consist of plutonic, volcanic and sedimentary rocks [22,24,25,41–44] and overlain by the Cenozoic units consisting of plutonic, volcanic and sedimentary rocks [7,9,50–54,26,29,30,45–49]. The youngest units in the region are Quaternary alluvium and terraces.

Corresponding author:
Email: abdullah.kaygusuz@gmail.com

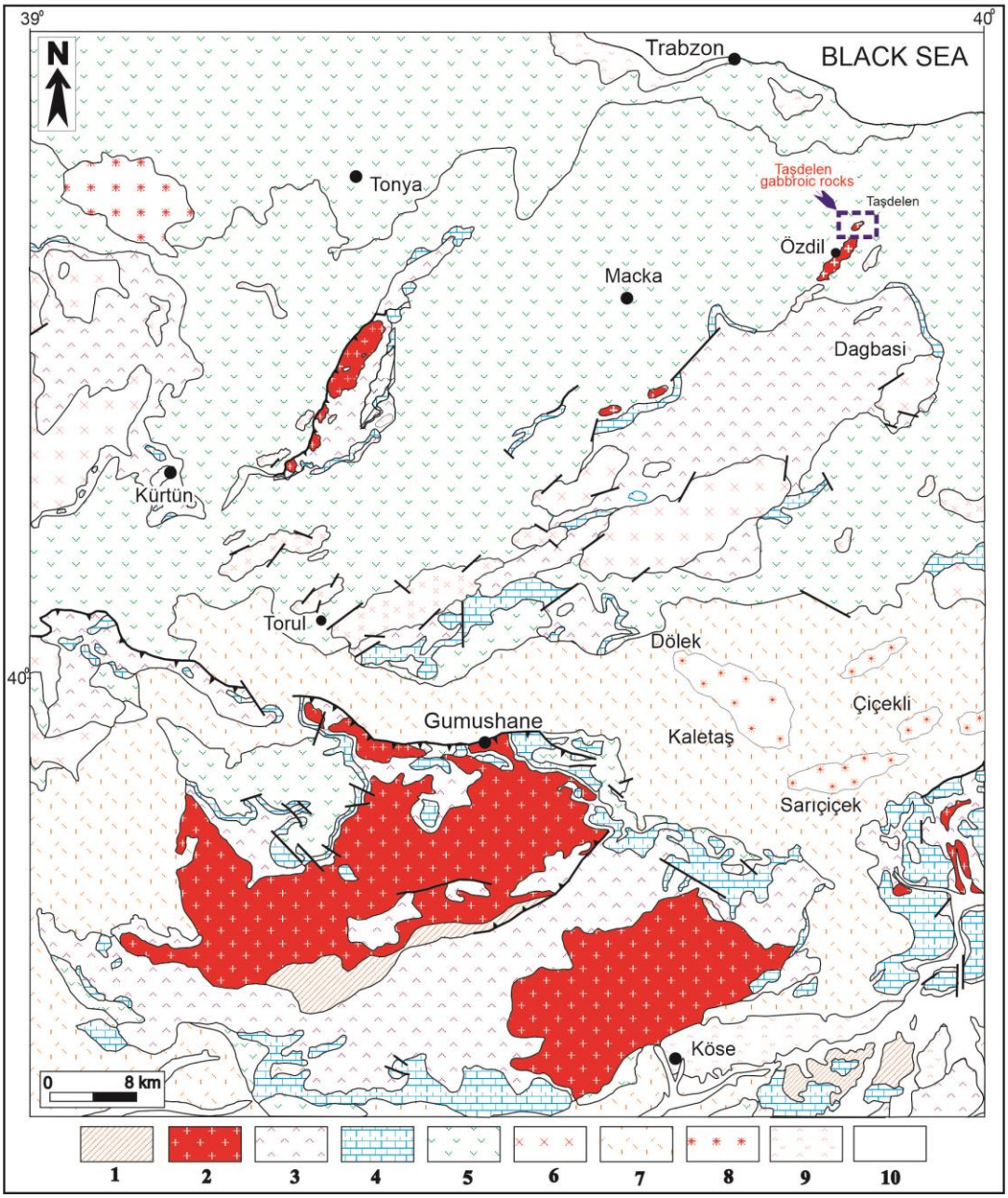

Figure 1. Geologic map showing distribution of plutonic, volcanic, metamorphic and sedimentary units in the Eastern Pontides (modified from [31]. (1) Palaeozoic metamorphic rocks, (2) Palaeozoic plutons, (3) Liassic–Dogger volcanic rocks, (4) Malm–Early Cretaceous sedimentary rocks, (5) Late Cretaceous volcanic rocks, (6) Late Cretaceous plutons, (7) Tertiary calc-alkaline volcanic rocks, (8) Tertiary alkaline volcanic rocks, (9) Eocene plutons, (10) alluvium

The study area is located in the north zone of the Eastern Pontides and is generally dominated by volcanic, plutonic and sedimentary rocks (Figure 1).

The basement rocks in the study area consist of Paleozoic Özdil Pluton which is monzonite, quartz monzonite and granite in compositions [16]. These basement rocks are unconformably overlain by Liassic volcanic rocks consisting of basalts, andesites and their pyroclastic equivalents. These rocks are overlain conformably by Late Cretaceous volcanic rocks that include andesite, dacite and their pyroclastics. All of these lithologies are cut by Late Cretaceous plutons. Eocene volcanic rocks that consist of andesite, basalt and their pyroclastics unconformably overlie all of these rocks (Figure 1).

3. Analysis methods

On the basis of field studies, a total of ten samples were collected from the studied Taşdelen gabbroic rocks in the fields. Thin sections of rock samples were made, and detailed petrographic properties were

determined under polarizing microscope. Fresh and representative rock samples were selected for whole-rock major, trace and rare earth element (REE) analyses. These analyses were made in ACME (Vancouver, Canada) Analytical Chemistry Laboratory. Major and trace elements were analyzed by ICP method, and rare earth elements (REE) by ICP-MS method. For the major and trace element analyses, 0.2 grams of powder sample was mixed with 1.5 grams of $LiBO_2$ and analyzed after dissolving in a liquid containing 5% HNO_3, while 0.250 grams of powder sample for rare earth element analyses was dissolved in four different acids and analyzed. Detection limits range from 0.002 to 0.04 wt% for major oxides, 0.1 to 8 ppm for trace elements, and 0.01 to 0.3 ppm for REE.

4. Results

4.1. Petrography

The Taşdelen gabbroic rocks are gabbro in compositions in the modal QAP diagram [55] (not shown). These gabbroic rocks are generally holocrystalline, medium to coarse grained, and large hornblends are of poikilitic texture. Main minerals are plagioclase, pyroxene, hornblende and Fe-Ti oxides (Figure 2).

Plagioclases form euhedral and subhedral lath-shaped phenocrysts. Some of which are partly replaced by clays, and some contain minor sericite. Clino-pyroxenes are found as subhedral to anhedral, weakly-zoned discrete grains and also in aggregates. Hornblends are in the form of elongated euhedral prismatic crystals and contain small apatite and opaque minerals as inclusions. They have well developed cleavages. Subhedral to anhedral apatites are relatively abundant accessory minerals. Zircons are seen as small euhedral prismatic crystals. Opaque minerals are found as subhedral and euhedral in both small and large crystals (Figure 2).

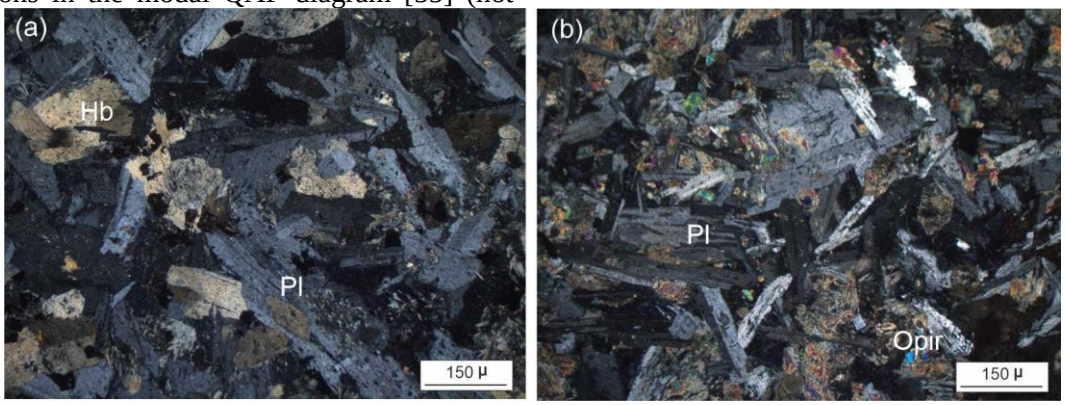

Figure 2. (a-b) Microscopic features of the studied Paleozoic Gabbroic rocks (crossed polars, Pl: plagioclase, Hb: hornblende, Opir: Ortho-pyroxene)

5. Whole-rock geochemistry

The whole-rock major, trace and rare earth element analysis results of five samples from the studied plutonic rocks are given in Table 1 and 2.

Taşdelen gabbroic rocks have low SiO_2 values (47-50 wt.%) and K_2O/Na_2O ratios (0.03-0.05, Table 2). The magnesium numbers [$Mg\#=100*(MgO/MgO+Fe_2O_3^T)$] of the samples vary between 54 and 57 (Table 2).

Table 1. The whole-rock major and trace element analysis of the studied Taşdelen gabbroic rocks

Sample number	1	2	3	4	5
Rock type	gabbro	gabbro	gabbro	gabbro	gabbro
SiO_2	47.47	48.09	48.88	49.08	49.59
TiO_2	1.96	1.75	1.83	1.52	1.44
Al_2O_3	15.48	15.63	16.79	16.65	16.89
$Fe_2O_3^T$	12.53	12.42	12.34	12.37	12.22
MnO	0.17	0.17	0.16	0.16	0.16
MgO	7.58	7.53	6.98	6.62	6.60
CaO	6.93	6.89	6.58	6.59	6.54
Na_2O	4.23	4.27	4.52	4.45	4.39
K_2O	0.11	0.12	0.14	0.16	0.20

P_2O_5	0.18	0.17	0.19	0.17	0.13
LOI	3.20	2.80	1.40	2.10	1.70
Total	99.84	99.84	99.81	99.87	99.86
Ni	23.40	21.20	18.70	18.20	12.60
V	319.00	326.00	333.00	344.00	357.00
Cu	61.30	30.30	4.40	4.20	2.10
Pb	1.10	1.35	1.23	1.92	1.85
Zn	35.00	33.00	24.00	16.00	15.00
W	0.50	0.50	0.90	0.70	1.00
Rb	10.40	10.30	11.60	11.90	12.50
Ba	62.00	63.00	66.00	65.00	74.00
Sr	360.60	358.80	338.30	339.20	322.10
Ta	0.30	0.30	0.50	0.50	0.40
Nb	4.40	4.60	5.50	5.10	6.20
Hf	3.20	3.10	3.40	3.60	3.80
Zr	113.80	117.20	139.80	143.90	148.10
Y	30.80	32.50	38.20	40.30	36.30
Th	0.70	0.80	1.10	1.00	1.30
U	0.20	0.20	0.30	0.30	0.20
Ga	14.60	15.80	17.40	17.90	18.40
K_2O/Na_2O	0.03	0.03	0.03	0.04	0.05
Mg #	57.11	57.17	55.46	54.09	54.32
A /CNK	0.79	0.79	0.86	0.85	0.87
Ce/Pb	27.64	23.04	26.42	17.24	18.27
Nb/La	0.34	0.36	0.41	0.35	0.42
Mg# (mg-number) = molar 100xMgO/(MgO+ $Fe_2O_3^T$). LOI is loss on ignition					

Table 2. The rare earth element analysis of the studied Taşdelen gabbroic rocks

Sample number	1	2	3	4	5
La	12.80	12.90	13.40	14.50	14.70
Ce	30.40	31.10	32.50	33.10	33.80
Pr	3.46	3.35	3.72	3.56	3.37
Nd	14.50	15.50	15.00	16.50	15.30
Sm	4.11	4.35	5.36	5.17	4.67
Eu	1.48	1.52	1.85	1.83	1.71
Gd	4.93	5.14	6.20	6.37	5.96
Tb	0.84	0.92	1.09	1.07	1.06
Dy	5.75	6.21	7.15	7.42	6.52
Ho	1.23	1.10	1.46	1.38	1.34
Er	3.74	3.35	4.30	4.22	3.82
Tm	0.50	0.51	0.62	0.63	0.58
Yb	2.82	2.98	3.50	3.56	3.68
Lu	0.42	0.49	0.58	0.60	0.56
$(Eu/Eu^*)_N$	1.00	0.98	0.98	0.97	0.99
$(La/Lu)_N$	3.16	2.73	2.39	2.50	2.72
$(La/Sm)_N$	1.96	1.87	1.57	1.77	1.98
$(Gd/Lu)_N$	1.46	1.30	1.33	1.32	1.32
$(La/Yb)_N$	3.07	2.93	2.59	2.75	2.70
$Eu^*=(Sm+Gd)_N/2$					

In the SiO_2 versus (Na_2O+K_2O) diagram (Figure 3a), the studied samples are gabbro in composition. Rock samples are in the low-K field in the K_2O versus SiO_2 diagram [56] (Figure 3b).

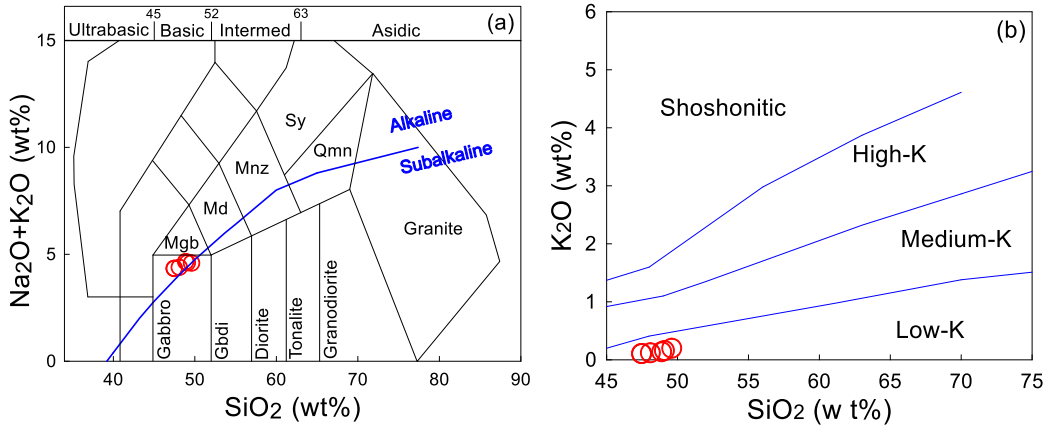

Figure 3. The studied Taşdelen gabbroic rocks; a) Chemical nomenclature diagram [57], b) K_2O versus SiO_2 diagram (field boundaries between the medium-K, high-K and shoshonitic series, according to [56]

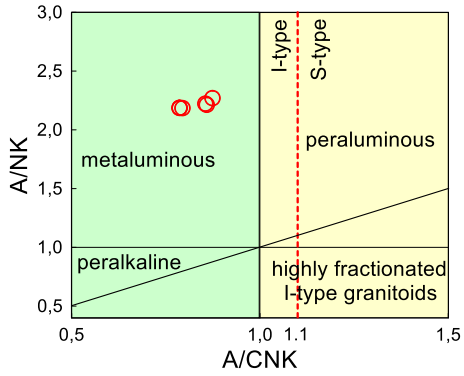

Figure 4. A/NK versus A/CNK diagram [58] of the studied Taşdelen gabbroic rocks

The A/CNK values of the samples are between 0.79 and 0.87, and they show metaluminous characters (Figure 4).

Although irregular distributions are observed in some of the major and trace elements versus SiO_2 diagrams (Figures 5 and 6), they give good correlations indicating that fractional crystallization plays an important role in the development of rocks. In the SiO_2 versus major element diagrams, Na_2O, CaO, MgO, Al_2O_3, $Fe_2O_3^T$, TiO_2 and P_2O_5 values decrease with increasing SiO_2 values (Figure 5). A positive correlation is observed in K_2O and Al_2O_3 versus SiO_2 diagram (Figure 5).

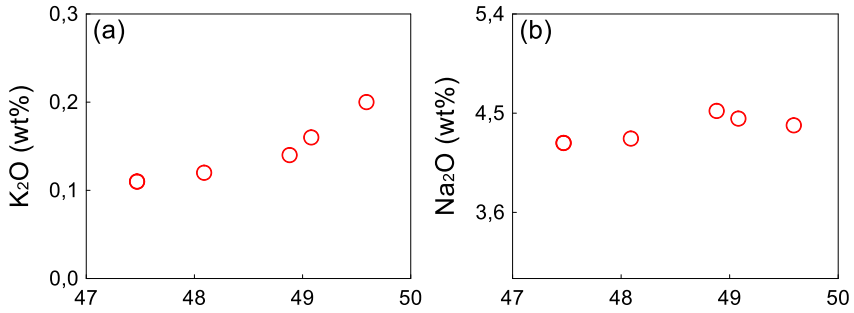

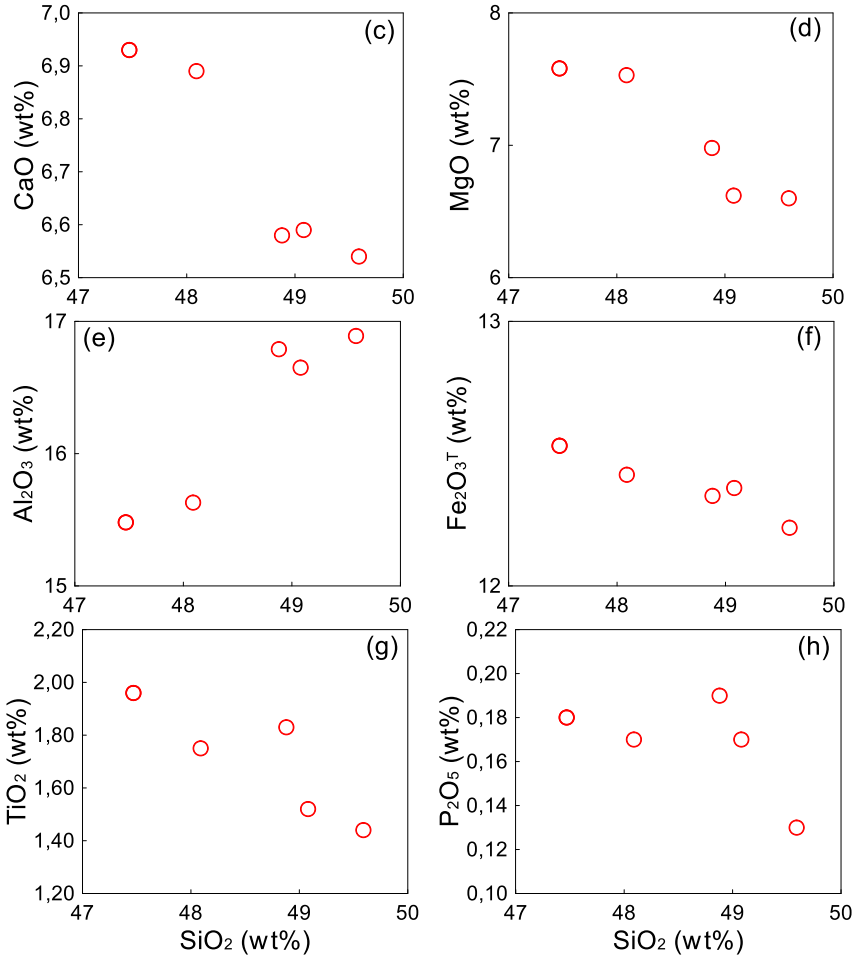

Figure 5. Variation diagrams of major oxides (wt.%) versus SiO_2 (wt.%) for the studied Taşdelen gabbroic rocks

In the trace element versus SiO_2 diagrams (Figure 6), a positive correlation is observed in Ba, Zr, Rb, Th, Y and Nb values, whereas a negative correlation is observed for Sr and Ni contents with increasing SiO_2 (Figure 6).

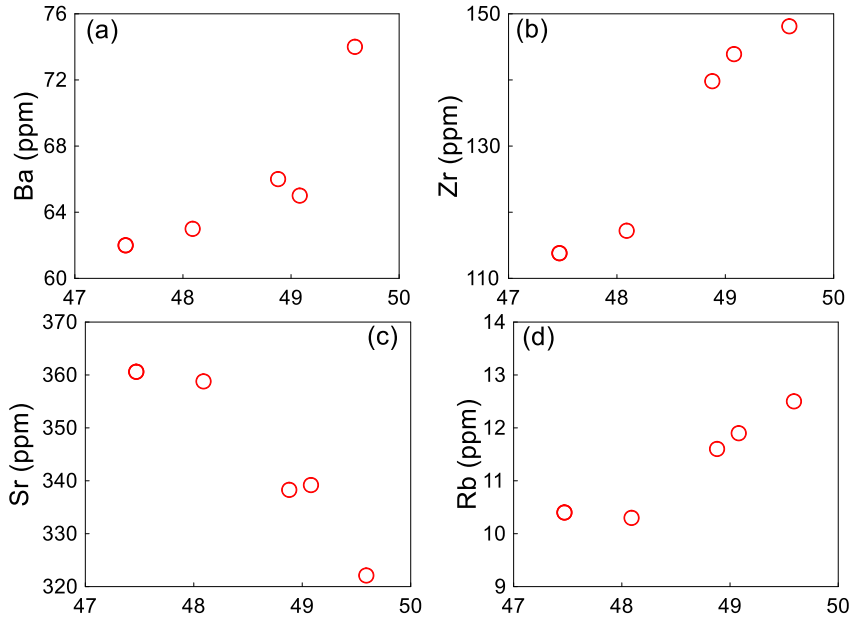

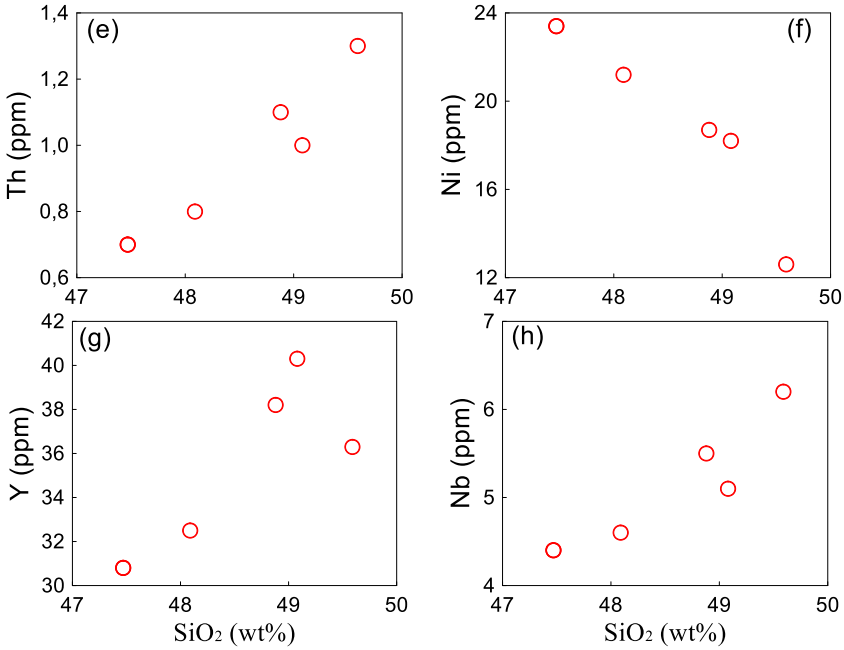

Figure 6. Variation diagrams of trace elements (ppm) versus SiO_2 (wt.%) for the studied Taşdelen gabbroic rocks

In the primitive mantle-normalized [59] multi-element variation diagrams (Figure 7a), all of the samples display similar patterns and differ from N-MORB and OIB. The samples show enrichment in large-ion lithophile elements (LILEs) and high field-strength elements (HFSEs). In the chondrite-normalized rare earth element (REE) distributions [60] diagrams (Figure 7b), as shown in Table 2, the studied rocks have relatively uniform contents of total rare earth elements (REEs). All of the samples exhibit enrichment in LREEs, depletion in HREEs, and no fractionation in HREEs but fractionation in LREEs (Figure 7b). The samples have slightly positive to negative Eu anomalies with a Eu/Eu* range from 0.97 to 1.00. $(La/Lu)_N$ ratios of the samples vary between 2.39 and 3.16; $(Gd/Lu)_N$ ratios vary between 1.32 and 1.46, and the $(La/Yb)_N$ ratios are between 2.59 and 3.07 (Table 2). As shown in Figure 7, the studied rocks are generally similar to each other, indicating that the rocks were derived from a similar source.

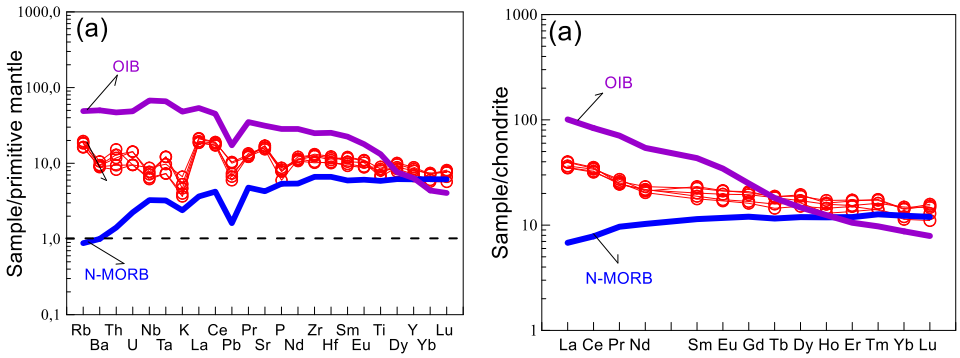

Figure 7. (a) Primitive mantle-normalized [59] trace element patterns, (b) Chondrite-normalized [60] rare earth element patterns of the studied Taşdelen gabbroic rocks

In the molar ASI (A/CNK) versus SiO_2 diagram of [61], all the samples are located in the field of I-type (Figure 8a). In the Nb versus 10000Ga/Al diagram developed by [62], all the samples are located in the I-type granite field (Figure 8b).

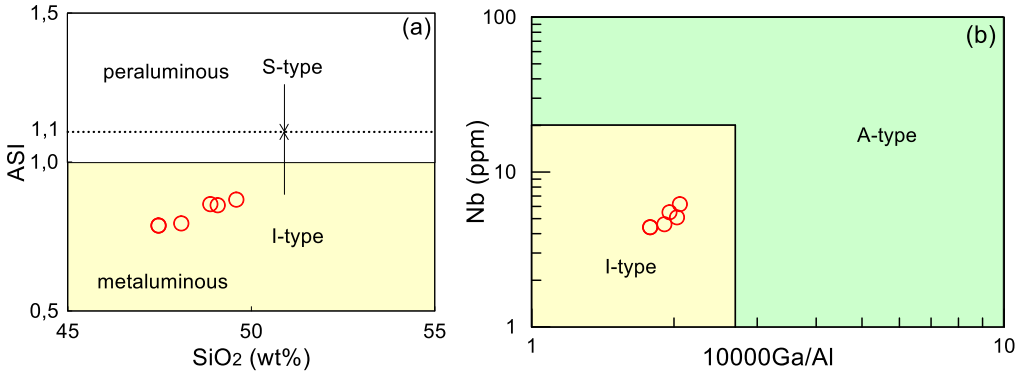

Figure 8. (a) ASI versus SiO_2 diagram [61], (b) Nb versus 10000 Ga/Al classification diagram [62] for the studied Taşdelen gabbroic rocks

In the Rb versus (Y+Nb) diagram of [63], the studied samples are located close to the triple intersection point of volcanic arc granitoids (VAG), intraplate granitoids (WPG) and syn-collision granitoids (Syn-COLG) fields (Figure 9a) characterized the post-collisional granitoids (Post-COLG). In the $(Nb/Zr)_N$ versus Zr diagram [58], most samples are located in the collision-related field (Figure 9b).

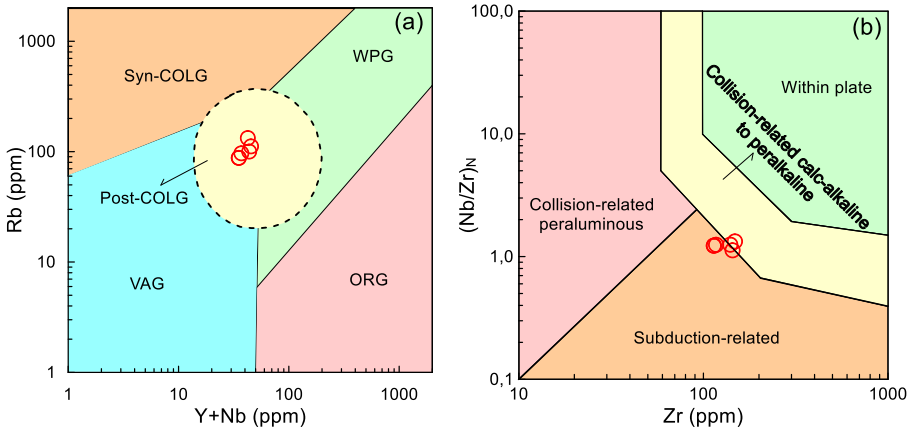

Figure 9. (a) Distributions of Rb versus (Y+Nb) in the tectono-magmatic diagram [63], (b) Zr versus $(Nb/Zr)_N$ diagram [58] for the studied Taşdelen gabbroic rocks

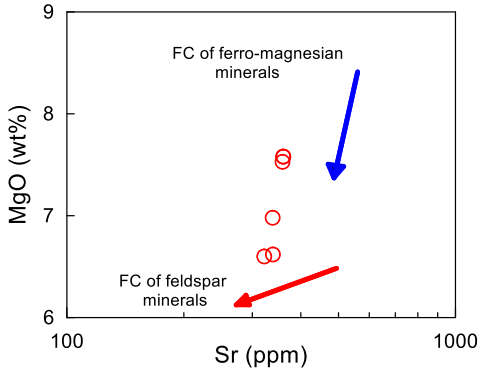

Figure 10. MgO versus Sr diagram for the studied Taşdelen gabbroic rocks

6. Discussion

The MgO values vary between 6.60 and 7.58%, Mg numbers (Mg#) between 54 and 57, and Ni values between 13 and 23 (ppm) of the studied Taşdelen gabbroic rocks (Table 1). These values indicate that the Taşdelen gabbroic rocks differ significantly from magmas derived from the primitive mantle composition (Mg# = ~ 66 to 75, Ni = ~ 400 to 500 ppm; [64]).

The distribution pattern of the some major and trace elements versus SiO_2 (SiO_2 increases with K_2O and Rb; TiO_2, Al_2O_3, Fe_2O_3, MgO, CaO and P_2O_5 decrease with increases SiO_2) of the studied samples (Figures 5 and 6) support plagioclase + hornblende + pyroxene + Fe-Ti oxide fractionations. The MgO versus Sr diagram (Figure 10) indicates fractionation of ferro-magnesian minerals.

The studied samples have low Ce/Pb ratios of 17-28 (Table 1) and differ from oceanic basalts (20 to 30) [65], indicating that the studied rocks did not derive from an asthenospheric mantle source. Nb/La ratios are useful in determining the partial melting and source composition of the rocks [66]. Low Nb/La ratios (<0.5) indicate a lithospheric mantle source, and high Nb/La ratios (>1) indicate an ocean island basalt (OIB)-like asthenospheric mantle source [67]. The Nb/La ratios of the studied rocks range from 0.34 to 0.42 (Table 1), indicating a lithospheric mantle source (Figure 11).

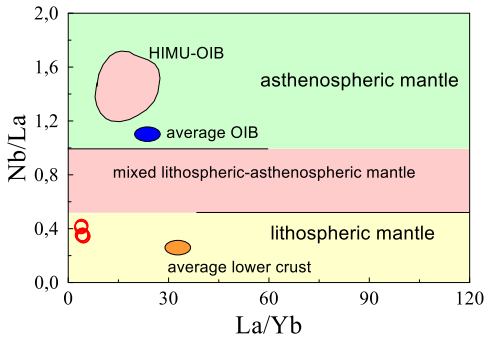

Figure 11. Nb/La versus La/Yb diagram for the studied Taşdelen gabbroic rocks. For reference values in diagrams, see Figure 13a caption in [4].

7. Conclusions

1. The studied gabbroic rocks are gabbro in composition defining low-K calc-alkaline series.
2. The samples have metaluminous characters and have low SiO_2 contents (47-49 wt%).
3. All of the samples display similar geochemical features characterized by enrichment in LILEs and LREEs, with pronounced depletion in HFSEs indicating similar sources and petrogenetic processes.
4. The main solidification processes involved in the evolution of the gabbroic rocks consist of fractional crystallization.
5. The studied gabbroic rocks were derived from partial melting of lithospheric mantle.

Acknowledgements

We thank the editor and referee for contributions to this study.

References

[1] Akaryalı E. Geochemical, fluid inclusion and isotopic (O, H and S) constraints on the origin of Pb–Zn±Au vein-type mineralizations in the Eastern Pontides Orogenic Belt (NE Turkey). Ore Geol Rev 2016; 74:1–14.

[2] Arslan M, Temizel İ, Abdioğlu E, Kolaylı H, Yücel C, Boztuğ D, Şen C. 40Ar–39Ar dating, whole-rock and Sr–Nd–Pb isotope geochemistry of post-collisional Eocene volcanic rocks in the southern part of the Eastern Pontides (NE Turkey): implications for magma evolution in extension-induced origin. Contrib to Mineral Petrol 2013; 166:113–142.

[3] Aydınçakır E, Yücel C, Ruffet G, Gücer MA, Akaryalı E, Kaygusuz A. Petrogenesis of post-collisional Middle Eocene volcanism in the Eastern Pontides (NE, Turkey): Insights from geochemistry, whole-rock Sr-Nd-Pb isotopes, zircon U-Pb and 40Ar-39Ar geochronology. Geochemistry 2022:125871.

[4] Kaygusuz A, Arslan M, Temizel İ, Yücel C, Aydınçakır E. U–Pb zircon ages and petrogenesis of the Late Cretaceous I-type granitoids in arc setting, Eastern Pontides, NE Turkey. J African Earth Sci 2021; 174:104040.

[5] Kaygusuz A, Siebel W, Şen C, Satir M. Petrochemistry and petrology of I-type granitoids in an arc setting: The composite Torul pluton, Eastern Pontides, NE Turkey. Int J Earth Sci 2008; 97:739–764.

[6] Özdamar Ş. Geochemistry and geochronology of late Mesozoic volcanic rocks in the northern part of the Eastern Pontide Orogenic Belt (NE

Turkey): Implications for the closure of the Neo-Tethys Ocean. Lithos 2016; 248–251:240–256.
[7] Temizel İ, Arslan M, Yücel C, Abdioğlu Yazar E, Kaygusuz A, Aslan Z. Eocene tonalite–granodiorite from the Havza (Samsun) area, northern Turkey: adakite-like melts of lithospheric mantle and crust generated in a post-collisional setting. Int Geol Rev 2020; 62:1131–1158.
[8] Vural A, Kaygusuz A. Geochronology, petrogenesis and tectonic importance of Eocene I-type magmatism in the Eastern Pontides, NE Turkey. Arab J Geosci 2021; 14.
[9] Yücel C, Arslan M, Temizel İ, Abdioğlu E. Volcanic facies and mineral chemistry of Tertiary volcanics in the northern part of the Eastern Pontides, northeast Turkey: Implications for pre-eruptive crystallization conditions and magma chamber processes. Mineral Petrol 2014; 108:439–467.
[10] Karslı O, Şengün F, Dokuz A, Aydin F, Kandemir R, Kristoffersen M, Santos JF, Hofmann M, Duygu L. Early Cambrian S-type granites in the Sakarya Zone, NE Turkey: A record for transition from subduction to post-collisional extension deduced from U-Pb zircon age and Nd-Hf isotopes. Lithos 2022; 428–429.
[11] Yılmaz Y. Petrology and structure of the Gümüşhane Granite and surrounding rocks, North-Eastern Anatolia. PhD Thesis, Univ London 1972:260 p.
[12] Çoğulu E. Gümüşhane ve Rize granitik plutonlarının mukayeseli petrojeolojik ve jeokronolojik etüdü. Unpubl Diss Thesis, İstanbul Tech Univ 1975.
[13] Topuz G, Altherr R, Siebel W, Schwarz WH, Zack T, Hasözbek A, Barth M, Satir M, Şen C. Carboniferous high-potassium I-type granitoid magmatism in the Eastern Pontides: The Gümüşhane pluton (NE Turkey). Lithos 2010; 116:92–110.
[14] Dokuz A. A slab detachment and delamination model for the generation of Carboniferous high-potassium I-type magmatism in the Eastern Pontides, NE Turkey: The Köse composite pluton. Gondwana Res 2011; 19:926–944.
[15] Kaygusuz A, Arslan M, Siebel W, Sipahi F, Ilbeyli N. Geochronological evidence and tectonic significance of Carboniferous magmatism in the southwest Trabzon area, eastern Pontides, Turkey. Int Geol Rev 2012; 54:1776–1800.
[16] Kaygusuz A, Arslan M, Sipahi F, Temizel İ. U–Pb zircon chronology and petrogenesis of Carboniferous plutons in the northern part of the Eastern Pontides, NE Turkey: Constraints for Paleozoic magmatism and geodynamic evolution. Gondwana Res 2016; 39:327–346.
[17] Kaygusuz A, Aydınçakır E, Yücel C, Atay HE. Petrographic and geochemical characteristics of carboniferous plutonic rocks around Erenkaya (Gümüşhane, NE Turkey). J Eng Res Appl Sci 2021; 10:1774–1778.
[18] Karslı O, Dokuz A, Kandemir R. Subduction-related Late Carboniferous to Early Permian Magmatism in the Eastern Pontides, the Camlik and Casurluk plutons: Insights from geochemistry, whole-rock Sr–Nd and in situ zircon Lu–Hf isotopes, and U–Pb geochronology. Lithos 2016; 266–267:98–114.
[19] Kaygusuz A. Geochronological age relationships of Carboniferous Plutons in the Eastern Pontides (NE Turkey). J Eng Res Appl Sci 2020; 9:1299–1307.
[20] Dokuz A, Karslı O, Chen B, Uysal I. Sources and petrogenesis of Jurassic granitoids in the Yusufeli area, Northeastern Turkey: Implications for pre- and post-collisional lithospheric thinning of the eastern Pontides. Tectonophysics 2010; 480:259–279.
[21] Aydınçakır E, Gündüz R, Yücel C. Emplacement conditions of magma(s) forming Jurassic plutonic rocks in Gümüşhane (Eastern Pontides, Turkey). Bull Miner Res Explor 2020; 162:175–196.
[22] Köprübaşı N, Şen C, Kaygusuz A. Doğu Pontid adayayı granitoyidlerinin karşılaştırılmalı petrografik ve kimyasal özellikleri, KD Türkiye. Uygulamalı Yerbilim Derg 2000; 1:111–120.
[23] Yılmaz S, Boztuğ D. Space and time relations of three plutonic phases in the Eastern Pontides, Turkey. Int Geol Rev 1996; 38:935–956.
[24] Aydın F, Oğuz Saka S, Şen C, Dokuz A, Aiglsperger T, Uysal İ, Kandemir R, Karslı O, Sarı B, Başer R. Temporal, geochemical and geodynamic evolution of the Late Cretaceous subduction zone volcanism in the eastern Sakarya Zone, NE Turkey: Implications for mantle-crust interaction in an arc setting. J Asian Earth Sci 2020; 192:104217.
[25] Kaygusuz A, Yücel C, Arslan M, Temizel İ, Yi K, Jeong YJ, Siebel W, Sipahi F. Eocene I-type magmatism in the Eastern Pontides, NE Turkey: insights into magma genesis and magma-tectonic evolution from whole-rock geochemistry, geochronology and isotope systematics. Int Geol Rev 2020; 62:1406–1432.
[26] Karslı O, Chen B, Aydın F, Şen C. Geochemical and Sr-Nd-Pb isotopic compositions

of the Eocene Dölek and Sariçiçek Plutons, Eastern Turkey: Implications for magma interaction in the genesis of high-K calc-alkaline granitoids in a post-collision extensional setting. Lithos 2007; 98:67–96.

[27] Temizel İ, Abdioğlu Yazar E, Arslan M, Kaygusuz A, Aslan Z. Mineral chemistry, whole-rock geochemistry and petrology of Eocene I-type shoshonitic plutons in the Gölköy area (Ordu, NE Turkey). Bull Miner Res Explor 2018; 157:121–152.

[28] Sipahi F, Saydam Eker Ç, Akpınar İ, Gücer MA, Vural A, Kaygusuz A, Aydurmuş T. Eocene magmatism and associated Fe-Cu mineralization in northeastern Turkey: a case study of the Karadağ skarn. Int Geol Rev 2022; 64:1530–1555.

[29] Eyuboğlu Y, Dudas FO, Thorkelson D, Zhu DC, Liu Z, Chatterjee N, Yi K, Santosh M. Eocene granitoids of northern Turkey: Polybaric magmatism in an evolving arc–slab window system. Gondwana Res 2017; 50:311–345.

[30] Kaygusuz A, Yücel C, Arslan M, Sipahi F, Temizel İ, Çakmak G, Güloglu ZS. Petrography, mineral chemistry and crystallization conditions of cenozoic plutonic rocks located to the north of Bayburt (Eastern Pontides, Turkey). Bull Miner Res Explor 2018; 157:75–102.

[31] Güven İH. Doğu Pontidlerin 1:25000 ölçekli kompilasyonu. MTA Genel Müdürlüğü 1993.

[32] Vural A, Kaygusuz A. Petrology of the paleozoic plutons in Eastern pontides: artabel pluton (Gümüşhane, NE Turkey). J Eng Res Appl Sci 2019; 8:1216–1228.

[33] Ustaömer T, Robertson AHF, Ustaömer PA, Gerdes A, Peytcheva I. Constraints on variscan and cimmerian magmatism and metamorphism in the pontides (Yusufeli-Artvin area), NE Turkey from U-Pb dating and granite geochemistry. Geol Soc Spec Publ 2013; 372:49–74.

[34] Dokuz A, Gücer MA, Karslı O, Yi K. From Cadomian back-arc basin to Rheic Ocean closure: the geochronological records of the Kurtoğlu Massif, eastern Sakarya Zone, Turkey. Int J Earth Sci 2022.

[35] Topuz G, Altherr R, Kalt A, Satir M, Werner O, Schwarz WH. Aluminous granulites from the Pulur complex, NE Turkey: A case of partial melting, efficient melt extraction and crystallisation. Lithos 2004; 72:183–207.

[36] Gücer MA, Arslan M, Sherlock S, Heaman LM. Permo-Carboniferous granitoids with Jurassic high temperature metamorphism in Central Pontides, Northern Turkey. Mineral Petrol 2016; 110:943–964.

[37] Kandemir R, Yılmaz C. Lithostratigraphy, facies, and deposition environment of the Lower Jurassic Ammonitico Rosso type sediments (ARTS) in the Gümüşhane area, NE Turkey: Implications for the opening of the northern branch of the Neo-Tethys Ocean. J Asian Earth Sci 2009; 34:586–598.

[38] Saydam Eker Ç, Sipahi F, Kaygusuz A. Trace and rare earth elements as indicators of provenance and depositional environments of Lias cherts in Gumushane, NE Turkey. Geochemistry 2012; 72:167–177.

[39] Eyuboğlu Y, Dudas FO, Santosh M, Xiao Y, Yi K, Chatterjee N, Wu FY, Bektaş O. Where are the remnants of a Jurassic ocean in the eastern Mediterranean region? Gondwana Res 2016; 33:63–91.

[40] Pelin S. Alucra (Giresun) Güneydoğu Yöresinin Petrol Olanakları Bakımından Jeolojik İncelenmesi. Karadeniz Tek Üniversitesi Yayınları 1977:87–103.

[41] Vural A, Kaygusuz A, Akpınar İ. Petrological characteristics of late Cretaceous volcanic rocks of Demirören (Gümüşhane, NE Turkey) region. J Eng Res Appl Sci 2021; 10:1828–1842.

[42] Vural A, Kaygusuz A. Petrographic and geochemical characteristics of late cretaceous volcanic rocks in the vicinity of Avliyana (Gümüşhane, NE Turkey). J Eng Res Appl Sci 2021; 10:1796–1810.

[43] Temizel İ, Arslan M, Abdioğlu Yazar E, Aslan Z, Kaygusuz A, Baki Eraydın T. Zircon U-Pb geochronology and petrology of the tholeiitic gabbro from the Kovanlık (Giresun) area: Constraints for the Late Cretaceous bimodal arc magmatism in the Eastern Pontides Orogenic Belt, NE Turkey. Lithos 2022; 428–429.

[44] Saydam Eker Ç, Korkmaz S. Mineralogy and whole rock geochemistry of lzate Cretaceous sandstones from the eastern Pontides (NE Turkey). Neues Jahrb Fur Mineral Abhandlungen 2011; 188:235–256.

[45] Aslan Z, Arslan M, Temizel İ, Kaygusuz A. K-Ar dating, whole-rock and Sr-Nd isotope geochemistry of calc-alkaline volcanic rocks around the Gümüşhane area: Implications for post-collisional volcanism in the Eastern Pontides, Northeast Turkey. Mineral Petrol 2014; 108:245–267.

[46] Aydın F, Karslı O, Chen B. Petrogenesis of the Neogene alkaline volcanics with implications for post-collisional lithospheric thinning of the Eastern Pontides, NE Turkey. Lithos 2008; 104:249–266.

[47] Aydınçakır E. The petrogenesis of Early Eocene non-adakitic volcanism in NE Turkey: Constraints on the geodynamic implications. Lithos 2014; 208:361–377.
[48] Kaygusuz A, Merdan Tutar Z, Yücel C. Mineral chemistry, crystallization conditions and petrography of Cenozoic volcanic rocks in the Bahçecik (Torul/Gumushane) area, Eastern Pontides (NE Turkey). J Eng Res Appl Sci 2017; 6:641–651.
[49] Topuz G, Okay AI, Altherr R, Schwarz WH, Siebel W, Zack T, Satir M, Sen C. Post-collisional adakite-like magmatism in the Agvanis Massif and implications for the evolution of the Eocene magmatism in the Eastern Pontides (NE Turkey). Lithos 2011; 125:131–150.
[50] Yücel C, Arslan M, Temizel İ, Abdioğlu Yazar E, Ruffet G. Evolution of K-rich magmas derived from a net veined lithospheric mantle in an ongoing extensional setting: Geochronology and geochemistry of Eocene and Miocene volcanic rocks from Eastern Pontides (Turkey). Gondwana Res 2017; 45:65–86.
[51] Kaygusuz A, Yücel C, Aydınçakır E, Gücer MA, Ruffet G. 40Ar–39Ar dating, whole-rock and Sr-Nd isotope geochemistry of the Middle Eocene calc-alkaline volcanic rocks in the Bayburt area, Eastern Pontides (NE Turkey): Implications for magma evolution in an extension-related setting. Mineral Petrol 2022; 116:379–399.
[52] Kaygusuz A, Aslan Z, Aydınçakır E, Yücel C, Gücer MA, Şen C. Geochemical and Sr-Nd-Pb isotope characteristics of the Miocene to Pliocene volcanic rocks from the Kandilli (Erzurum) area, Eastern Anatolia (Turkey): Implications for magma evolution in extension-related origin. Lithos 2018; 296–299:332–351.
[53] Kaygusuz A, Şahin K. Petrographical, geochemical and petrological characteristics of Eocene volcanic rocks in the Mescitli area, Eastern Pontides (NE Turkey). J Eng Res Appl Sci 2016; 5:473–486.
[54] Saydam Eker Ç. Potentially toxic element levels in the Eocene sandstones from Gümüşhane area (NE Turkey). J Eng Res Appl Sci 2020.
[55] Streckeisen A. To each plutonic rock its proper name. Earth Sci Rev 1976; 12:1–33.
[56] Le Maitre RW, Bateman P, Dudek A, Keller J, Lameyre J, Le Bas MJ, Sabine PA, Schmid R, Sorensen H, Streckeisen A, Wooley AR, Zanettin B. A classification of igneous rocks and glossary of terms. Blackwell, Oxford 1989:193 pp.
[57] Middlemost EAK. Naming materials in the magma/igneous rock system. Earth Sci Rev 1994; 37:215–224.
[58] Maniar PD, Piccoli PM. Tectonic discrimination of granitoids. Geol Soc Am Bull 1989; 101:635–643.
[59] Sun SS, McDonough WF. Chemical and isotopic systematics of oceanic basalts: implications for mantle composition and processes. Geol Soc London, Spec Publ 1989; 42:313–345.
[60] Taylor SR, McLennan SM. The Continental Crust; Its Composition and Evolution. Geosci Text, Blackwell Sci Publ 1985.
[61] Chappell BW, White AJR. Two contrasting granite types. Pacific Geol 1974; 8:173–174.
[62] Whalen JB, Currie KL, Chappell BW. A-type granites: geochemical characteristics, discrimination and petrogenesis. Contrib to Mineral Petrol 1987; 95:407–419.
[63] Pearce JA, Harris NBW, Tindle AG. Trace element discrimination diagram for the tectonic interpretation of granitic rocks. J Petrol 1984; 25:956–983.
[64] Frey FA, Green D, Roy S. Integrated models of basalt of petrogenesis, a study of quartz tholeiites to olivine melilitites from south Australia utilizing geochemical and experimental petrological data. J Petrol 1978; 19:463–513.
[65] Hoffmann AW. Chemical differentiation of the Earth. The relationship between mantle, continental crust and oceanic crust. Earth Planet Sci Lett 1988; 90:297–314.
[66] Jahn BM, Wu FY, Lo CH. Crust-mantle interaction induced by deep subduction of the continental crust: geochemical and Sr-Nd isotopic evidence from post-collisional mafic-ultramafic intrusions of the northern Dabie Complex, Central China. Chem Geol 1999; 157:119–146.
[67] Smith EI, Sanchez A, Walker JD, Wang K. Geochemistry of mafic magmas in the Hurricane Volcanic field, Utah: implications for small- and large-scale chemical variability of the lithospheric mantle. J Geol 1999; 107:433–448.